# Seasonal to decadal variations of water vapor in the tropical lower stratosphere observed with balloon-borne cryogenic frost point hygrometers

M. Fujiwara,[1] H. Vömel,[2] F. Hasebe,[1] M. Shiotani,[3] S.-Y. Ogino,[4] S. Iwasaki,[5] N. Nishi,[6] T. Shibata,[7] K. Shimizu,[1,8] E. Nishimoto,[3] J. M. Valverde Canossa,[9] H. B. Selkirk,[10] and S. J. Oltmans[11]

Received 10 March 2010; revised 10 June 2010; accepted 22 June 2010; published 21 September 2010.

[1] We investigated water vapor variations in the tropical lower stratosphere on seasonal, quasi-biennial oscillation (QBO), and decadal time scales using balloon-borne cryogenic frost point hygrometer data taken between 1993 and 2009 during various campaigns including the Central Equatorial Pacific Experiment (March 1993), campaigns once or twice annually during the Soundings of Ozone and Water in the Equatorial Region (SOWER) project in the eastern Pacific (1998–2003) and in the western Pacific and Southeast Asia (2001–2009), and the Ticosonde campaigns and regular sounding at Costa Rica (2005–2009). Quasi-regular sounding data taken at Costa Rica clearly show the tape recorder signal. The observed ascent rates agree well with the ones from the Halogen Occultation Experiment (HALOE) satellite sensor. Average profiles from the recent five SOWER campaigns in the equatorial western Pacific in northern winter and from the three Ticosonde campaigns at Costa Rica (10°N) in northern summer clearly show two effects of the QBO. One is the vertical displacement of water vapor profiles associated with the QBO meridional circulation anomalies, and the other is the concentration variations associated with the QBO tropopause temperature variations. Time series of cryogenic frost point hygrometer data averaged in a lower stratospheric layer together with HALOE and Aura Microwave Limb Sounder data show the existence of decadal variations: The mixing ratios were higher and increasing in the 1990s, lower in the early 2000s, and probably slightly higher again or recovering after 2004. Thus linear trend analysis is not appropriate to investigate the behavior of the tropical lower stratospheric water vapor.

**Citation:** Fujiwara, M., et al. (2010), Seasonal to decadal variations of water vapor in the tropical lower stratosphere observed with balloon-borne cryogenic frost point hygrometers, *J. Geophys. Res.*, *115*, D18304, doi:10.1029/2010JD014179.

## 1. Introduction

[2] Water vapor in the stratosphere contributes to the radiative balance of the stratosphere and influences variability and recovery of the ozone layer through its radiative and photochemical nature [e.g., *Kley et al.*, 2000]. Its concentration is controlled by dehydration processes in the tropical tropopause layer (TTL) [*Fueglistaler et al.*, 2009], methane oxidation within the stratosphere [*Rohs et al.*, 2006], and transport associated with the diabatic meridional circulation, i.e. the Brewer-Dobson circulation [*Holton et al.*, 1995]. Variability of water vapor in the tropical lower stratosphere largely reflects dehydration processes occurring in the TTL, and therefore measurements and understanding of the variability are crucial for global atmospheric chemistry and climate.

[3] Seasonal variation of water vapor in the tropical lower stratosphere has been observed with satellite sensors, particularly the Halogen Occultation Experiment (HALOE) instrument on board the Upper Atmosphere Research

[1]Graduate School of Environmental Science, Hokkaido University, Sapporo, Japan.
[2]Meteorologisches Observatorium Lindenberg, Deutscher Wetterdienst, Lindenberg, Germany.
[3]Research Institute for Sustainable Humanosphere, Kyoto University, Uji, Japan.
[4]Japan Agency for Marine-Earth Science and Technology, Yokosuka, Japan.
[5]National Defense Academy, Yokosuka, Japan.
[6]Graduate School of Science, Kyoto University, Kyoto, Japan.
[7]Graduate School of Environmental Studies, Nagoya University, Nagoya, Japan.
[8]Also at Meisei Electric Co., Ltd., Isesaki, Japan.
[9]Universidad Nacional, Heredia, Costa Rica.
[10]Goddard Earth Sciences and Technology Center, University of Maryland Baltimore County, NASA Goddard Space Flight Center, Greenbelt, Maryland, USA.
[11]Global Monitoring Division, NOAA Earth System Research Laboratory, Boulder, Colorado, USA.


0148-0227/10/2010JD014179

Satellite (UARS) which was in operation between September 1991 and December 2005 [e.g., *Mote et al.*, 1996; *Randel et al.*, 2001]. Tropical tropopause temperatures have a prominent seasonal cycle, which primarily control the effective entry value of water vapor; the seasonally varying entry values then propagate upward in the tropical lower stratosphere by the ascending branch of the Brewer-Dobson circulation. The signature in water vapor is often termed as the tape recorder signal with the tape head at the tropical tropopause [*Mote et al.*, 1996].

[4] Short-term interannual variations of water vapor in the tropical lower stratosphere are mainly caused by the quasi-biennial oscillation (QBO) and El Niño–Southern Oscillation (ENSO). The QBO modulates the tropical lower stratospheric water vapor through the modulation of tropical tropopause temperatures and hence the effective entry value, and through the modulation of the tropical ascending speed of the Brewer-Dobson circulation. *Niwano et al.* [2003] used HALOE water vapor and methane data to estimate the QBO modulation of the Brewer-Dobson circulation quantitatively. *Randel et al.* [2004] and *Fueglistaler and Haynes* [2005] discussed that both the QBO and ENSO are the primary cause of interannual variations of the tropical tropopause temperature and the water vapor around the bottom of the tropical lower stratosphere.

[5] As for longer-term variations, linear increasing trends of stratospheric water vapor have been reported based on balloon-borne cryogenic frost point hygrometer data at a Northern Hemisphere midlatitude site, Boulder (40.00°N, 105.25°W), Colorado, since 1980 [*Oltmans et al.*, 2000; *Scherer et al.*, 2008] and based on 10 data sets including the Boulder data since 1954 [*Rosenlof et al.*, 2001]. The increasing rate is reported as ~0.6% per year for 1980–2000 [*Scherer et al.*, 2008] and ~1% per year (~0.05 parts per million by volume, ppmv, per year) for 1954–2000 [*Rosenlof et al.*, 2001]. These increasing trends have important implications for the ozone layer and climate [e.g., *Scherer et al.*, 2008, and references therein; *Solomon et al.*, 2010]. Around 2000–2001 a drop in lower stratospheric water vapor was observed, and since then, persistent low values have been observed at least up to 2005 based on the Boulder in situ data and HALOE data (around Boulder; in the tropics; and at 60°N–60°S) [*Randel et al.*, 2006; *Scherer et al.*, 2008]. The changes around 2000–2001 may imply the existence of decadal variations in the TTL and tropical lower stratosphere.

[6] The mechanisms responsible for the increasing trends during the past half-century and for the recent possible decadal variations are still unclear. The increase of methane can account for only ~30% of the increase in stratospheric water vapor [*Rohs et al.*, 2006]. Although the estimation of tropical tropopause temperature trends was found to be difficult due to frequent, often undocumented changes in radiosonde and satellite instrumentation, there could have been a cooling trend rather than a warming trend at least during the past two to three decades [e.g., *Rosenlof and Reid*, 2009, and references therein; *Seidel et al.*, 2009, Figure 4]. The apparent lack of mechanisms supporting the increasing trends prompted a search for other processes such as changes in the tropical ascending branch of the Brewer-Dobson circulation (i.e., its latitudinal width, and strength in season) [*Rosenlof*, 2002], detailed microphysical processes occurring in the dehydration within the TTL (which may disconnect the direct relation between temperature and water vapor) [e.g., *Sherwood*, 2002; *Peter et al.*, 2006], among others. However, there is no successful explanation for the increasing trends at present. *Fueglistaler and Haynes* [2005] discussed that the long-term trends might have been overestimated. As for the recent possible decadal variations, *Randel et al.* [2006] pointed out that intensification of the Brewer-Dobson circulation may have occurred after 2001. On the other hand, *Rosenlof and Reid* [2008] proposed a link among the sea surface temperatures and convective activity in the tropical western Pacific, tropical tropopause temperatures, and tropical lower stratospheric water vapor (note that *Lanzante* [2009] questioned some of their key findings specifically regarding the temperature observations used in their paper). Furthermore, there exist inconsistencies in trends and variability between the two key water vapor data sets, namely, the Boulder in situ data and HALOE data [*Randel et al.*, 2004; *Scherer et al.*, 2008].

[7] There have been several tropical campaigns since the early 1990s where the same types of balloon-borne cryogenic frost point hygrometers as those used at Boulder were flown (Figures 1 and 2 and Tables 1 and 2). Major campaigns are the Central Equatorial Pacific Experiment (CEPEX) campaign over the central equatorial Pacific Ocean in March 1993, campaigns once or twice annually under the Soundings of Ozone and Water in the Equatorial Region (SOWER) project at several tropical Pacific and Southeast Asian sites from 1998 to present, and campaigns and regular sounding activity under the Ticosonde project at Costa Rica in Central America from 2005 to present. The water vapor data taken during these tropical campaigns have been used for TTL dehydration studies [e.g., *Vömel et al.*, 1995a, 2002; *Fujiwara et al.*, 2001; *Hasebe et al.*, 2007; *Shibata et al.*, 2007; *Selkirk et al.*, 2010; *Inai*, 2010], satellite validation [e.g., *Vömel et al.*, 2007a], and radiosonde humidity sensor validation [e.g., *Vömel et al.*, 2003, 2007b]. However, these data have not yet been used for studies on seasonal to interannual variations.

[8] The purpose of this paper is to investigate seasonal to decadal variations of water vapor in the tropical lower stratosphere using in situ balloon-borne cryogenic frost point hygrometer data taken at various tropical sites over the last 17 years, 1993–2009 (Figure 1). As discussed above, water vapor variations in the tropical lower stratosphere have been investigated primarily with satellite sensors, particularly HALOE data. Analyses and comparisons are also made with satellite water vapor data from HALOE (up to 21 November 2005) and from the Microwave Limb Sounder (MLS) on board the NASA Earth Observing System (EOS) Aura satellite launched in July 2004. Tropical in situ data up to 2009 will provide some new insights into the tropical lower stratospheric water vapor behavior. The remainder of this paper is organized as follows. Section 2 describes the tropical balloon observations and satellite data sets, section 3 provides results and discussion on seasonal variations, QBO-related variations,

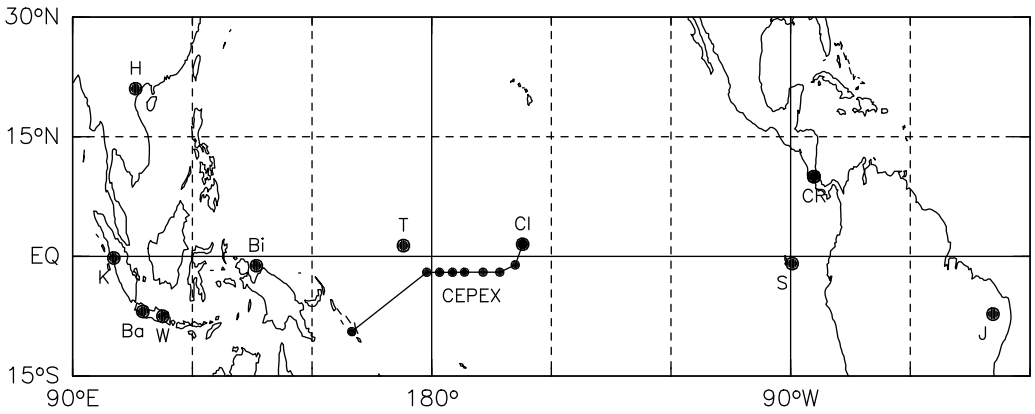


**Figure 1.** Location of the observation sites. H, Ha Noi (21.01°N, 105.80°E); K, Kototabang (0.20°S, 100.32°E); Ba, Bandung (6.90°S, 107.60°E); W, Watukosek (7.57°S, 112.65°E); Bi, Biak (1.17°S, 136.06°E); T, Tarawa (1.35°N, 172.92°E); CI, Christmas Island (1.52°N, 157.20°W); S, San Cristóbal Island (0.90°S, 89.62°W); CR, Alajuela (9.98°N, 84.21°W; July–September 2005, and May 2007 to present) and Heredia (10.00°N, 84.11°W; October 2005 to January 2007), Costa Rica; J, Juazeiro do Norte (7.23°S, 39.28°W). Smaller dots connected with lines indicate the sounding locations of the research vessel Vickers under the Central Equatorial Pacific Experiment (CEPEX).

and decadal variations, and finally, section 4 lists the main conclusions.

## 2. Observations and Data Description

### 2.1. Cryogenic Frost Point Hygrometers and Field Campaigns

[9] In this paper, we use data from two types of balloon-borne cryogenic frost point hygrometer, the National Oceanic and Atmospheric Administration (NOAA) cryogenic frost point hygrometer (NOAA FPH) (the analog controller versions) [*Vömel et al.*, 1995b; *Kley et al.*, 2000; *Vömel et al.*, 2007c] and the University of Colorado cryogenic frost point hygrometer (CFH) [*Vömel et al.*, 2007d]. These instruments are based on the chilled mirror principle and provide a direct measurement of the frost point temperature of the ambient air. The total uncertainty of the NOAA FPH above the middle-to-upper troposphere is estimated as ~0.5°C frost point temperature which translates to ~10% in lower stratospheric water vapor mixing ratio [*Vömel et al.*, 1995b]. The CFH is an upgraded version of the NOAA FPH and utilizes the advanced digital controller that allows continuous measurements of frost point/dew point temperature between the surface and the middle stratosphere. The total uncertainty of the CFH for the tropical mixing ratio measurements is estimated as 3%–5% in the lower-to-middle troposphere, 5%–8% in the upper troposphere and in the TTL, and 8%–9.5% in the lower stratosphere up to 28 km altitude [*Vömel et al.*, 2007d].

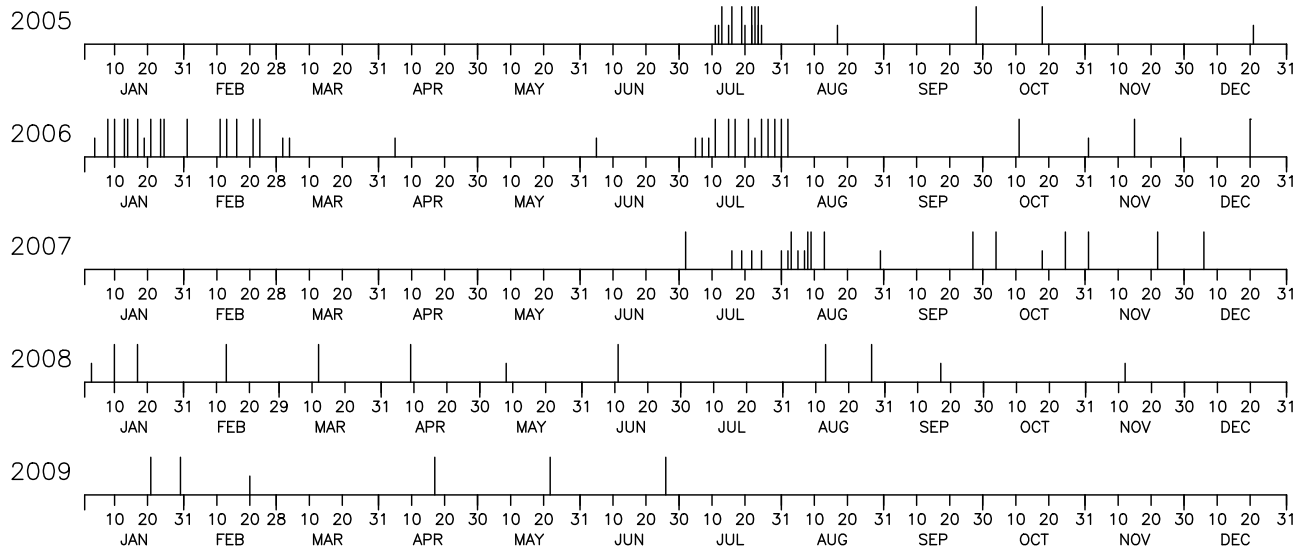


**Figure 2.** CFH sounding schedule at Costa Rica between July 2005 and June 2009 under the Ticosonde project. Half lines indicate successful soundings with good quality data points above the 100 hPa level but below the 37 hPa level. Full lines indicate those with good quality data points above the 37 hPa level (for Figure 11).

**Table 1.** List of Tropical NOAA Frost Point Hygrometer (NOAA FPH) Soundings After 1993

| Period | Place | Project | Total Number | Number[a] (37 hPa) |
|---|---|---|---|---|
| Mar 1993 | western/central Pacific to Christmas Island | CEPEX | 13 | 11 |
| Feb 1997 | Juazeiro do Norte, Brazil | NOAA | 1 | 1 |
| Nov 1997 | Juazeiro do Norte, Brazil | NOAA | 2 | 1 |
| Mar–Apr 1998 | San Cristóbal Island, the Galápagos | SOWER | 3 | 2 |
| Sep 1998 | San Cristóbal Island, the Galápagos | SOWER | 5 | 3 |
| Mar 1999 | San Cristóbal Island, the Galápagos | SOWER | 2 | 2 |
| Sep–Oct 1999 | San Cristóbal Island, the Galápagos | SOWER | 3 | 2 |
| Nov–Dec 2000 | San Cristóbal Island, the Galápagos | SOWER | 6 | 2 |
| Nov–Dec 2001 | Watukosek, Indonesia | SOWER | 5 | 0 |
| Aug 2002 | San Cristóbal Island, the Galápagos | NOAA | 2 | 2 |
| Jan 2003 | Watukosek, Indonesia | SOWER | 3 | 1 |
| Mar 2003 | San Cristóbal Island, the Galápagos | NOAA | 1 | 0 |

[a]Number of successful soundings with good quality data points above the 37 hPa level (for Figure 11).

[10] Vaisala RS80 radiosondes were used as data transmitters, which simultaneously provided measurements of pressure, temperature, and tropospheric relative humidity. The data sampling rate is at 8 s for the NOAA FPH and 1.2 s for the CFH, depending on the interface board used in the telemetry system. The uncertainty of the pressure measurement of this radiosonde used in this telemetry system is within 0.5 hPa.

[11] In both instruments, data were obtained both during ascent and descent. For the NOAA FPH measurements, mostly descent data are used due to the slightly larger contamination potential, and the data are averaged for every 250 m bin. For the CFH measurements, both ascent and descent data are being used; data suspected of contamination are flagged out (such data points are sometimes found above 20 km) (see sections 2.2 and 2.5 of and discussions by *Vömel et al.* [2007d]). In this paper, for the CFH measurements, the ascent data are primarily used, and vertical averages are taken (e.g., for ~250 m) where appropriate.

[12] Table 1 lists tropical NOAA FPH data taken within the CEPEX, SOWER, and NOAA projects. There was no campaign in 1994–1996, and the campaigns were mostly made in northern winter to spring except for the three campaigns at San Cristóbal Island. It should be noted that the NOAA FPH data taken in the CEPEX campaign were adjusted to the HALOE measurements to compensate for the radio frequency interference [*Vömel et al.*, 1995a]. Also, the low temperature calibration correction (below -79°C) described by *Vömel et al.* [2007c] and *Scherer et al.* [2008] has been applied to all NOAA FPH data except for those taken during the CEPEX campaign. For the 68–37 hPa layer averages that will be discussed in section 3.3, this correction procedure resulted in ~−0.06 ppmv (~−2%) corrections. Table 2 lists CFH data taken under the SOWER project. In 2003, we switched from NOAA FPH to CFH for the tropical campaigns (see section 2.9 of *Vömel et al.* [2007d] about the December 2003 campaign). After 2003, the SOWER campaigns were made in the tropical western Pacific to Southeast Asian region annually in northern winter. After 2007, we conducted campaigns at different locations simultaneously for the match analysis [*Inai*, 2010]. Figure 2 shows the CFH sounding schedule at Costa Rica between July 2005 and June 2009 under the Ticosonde project [*Selkirk et al.*, 2010]. The total number of CFH soundings in this period is 124. Figure 2 only shows the soundings with good quality data points above the 37 hPa (~23 km) level (58 in total) and above the 100 hPa (~16 km) level but below the 37 hPa level (36 in total). There were four intensive campaigns and once or twice monthly soundings, with some exceptions, to cover different seasons. It should be noted that soundings in Costa Rica were made at Alajuela (9.98°N, 84.21°W) from July to September 2005, at Heredia (10.00°N, 84.11°W) from October 2005 to January 2007, and again at Alajuela from May 2007, with the same operation team.

[13] For the analysis of seasonal variations, Ticosonde CFH profiles with good quality data points above the 100 hPa level will be used. For the analysis of QBO related variations, both Ticosonde and SOWER CFH profiles (above the 100 hPa level) after December 2004 will be used. For the analysis of longer-term variations (Figure 11), only the NOAA FPH and CFH profiles with good quality data points above the 37 hPa level will be used.

### 2.2. Satellite Measurements

[14] The HALOE instrument uses a solar occultation technique at near-infrared to infrared wavelengths to measure water vapor and other key constituents in the middle atmosphere [*Russell et al.*, 1993]. The measurements roughly span latitudes ~80°N–80°S and were taken between 11 October 1991 and 21 November 2005. The time and location of each vertical measurement depend on the satellite's near-polar orbit and the occultation configuration for sunrise and sunset. The number of measurements in the latitudes 10°N–10°S within a month varies from zero to ~60 for each sunrise and sunset occultation data set. *Harries et al.* [1996] estimated the accuracy of the version 17 water vapor data set as ±10% over most of the height range in the

**Table 2.** List of Tropical Cryogenic Frost Point Hygrometer (CFH) Soundings Under the SOWER Project

| Period | Place | Total Number | Number[a] (100 hPa) | Number[b] (37 hPa) |
|---|---|---|---|---|
| Dec 2003 | Bandung, Indonesia | 4 | 0 | 0 |
| Dec 2004 | Bandung, Indonesia | 4 | 4 | 1 |
| Dec 2005 | Tarawa, Kiribati | 2 | 0 | 0 |
| Jan 2006 | Biak, Indonesia | 9 | 8 | 5 |
| Jan 2007 | Biak, Indonesia | 6 | 6 | 5 |
| | Kototabang, Indonesia | 5 | 4 | 4 |
| | Tarawa, Kiribati | 5 | 4 | 4 |
| | Ha Noi, Vietnam | 6 | 6 | 6 |
| Jan 2008 | Biak, Indonesia | 7 | 7 | 5 |
| | Kototabang, Indonesia | 4 | 4 | 3 |
| | Ha Noi, Vietnam | 5 | 5 | 5 |
| Jan 2009 | Biak, Indonesia | 4 | 4 | 3 |
| | Ha Noi, Vietnam | 4 | 4 | 3 |

[a]Number of successful soundings with good quality data points above the 100 hPa level but below the 37 hPa level.

[b]Number of successful soundings with good quality data points above the 37 hPa level (for Figure 11).

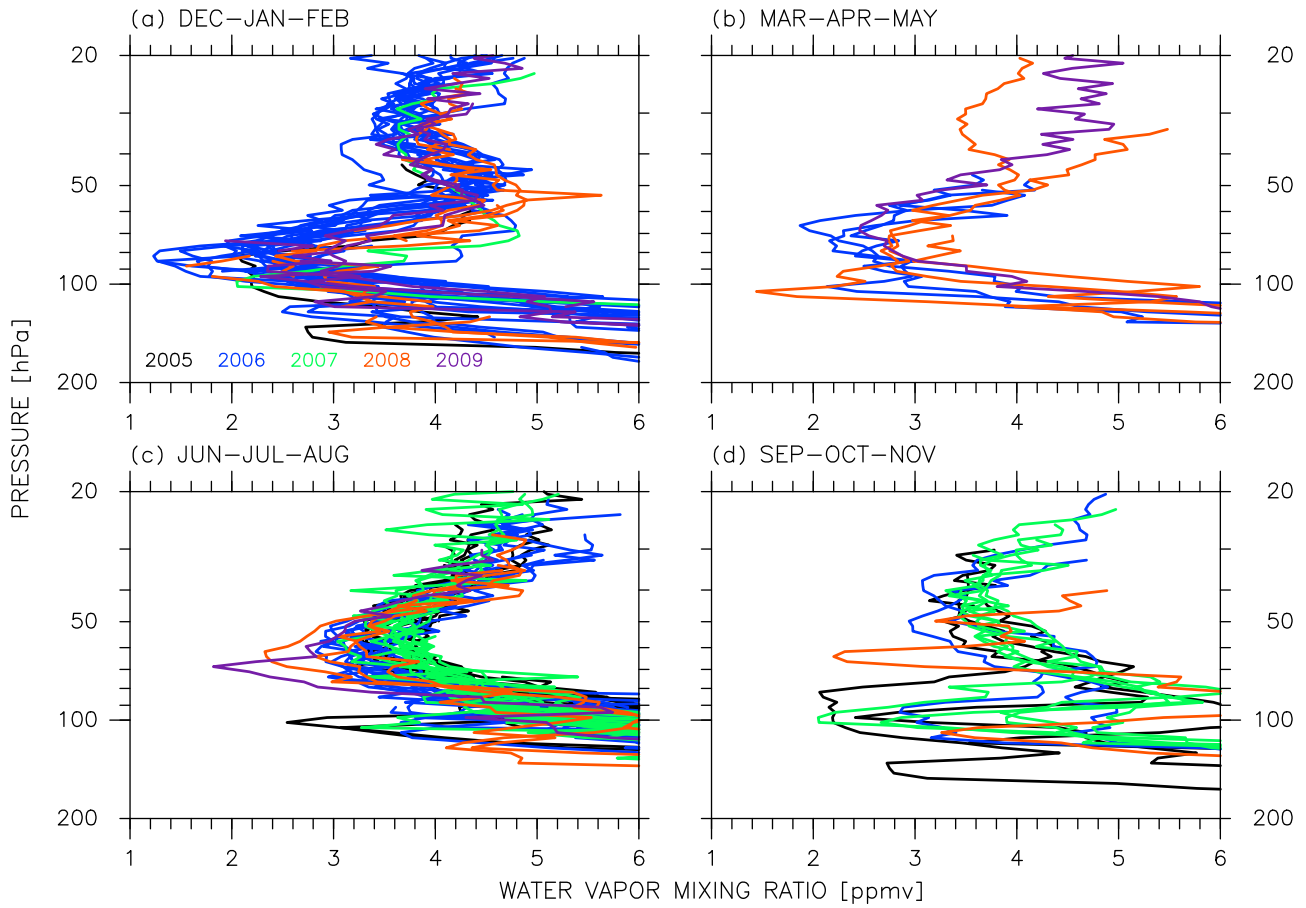


**Figure 3.** Water vapor mixing ratio profiles at Costa Rica in (a) December–January–February, (b) March–April–May, (c) June–July–August, and (d) September–October–November. Black curves are for measurements in 2005, blue for 2006, green for 2007, orange for 2008, and purple for 2009.

middle atmosphere and ±30% at the boundaries and the precision at a few percent in the lower stratosphere. In this paper, we use the HALOE version 19 data, file version P1.6 (downloaded from http://haloe.gats-inc.com/ in October 2008) with 30 standard levels per decade of pressure (e.g., 100.0, 92.61187, 85.76959, 79.43282,… hPa). Note that studies using HALOE water vapor data described in the Introduction used data version 17 or 18 or 19. For example, *Randel et al.* [2001, 2004, 2006] used data version 19 with a different standard pressure level set (12 standard levels per decade of pressure). As this manuscript was in preparation, data version 20 was being prepared at Hampton University (James M. Russell III, private communication, 2009). The major revisions include the consideration of temperature-dependent effects of the interfering $O_2$ continuum (see sections 1.4.5 and 2.3.1 of *Kley et al.* [2000]) and the use of 2.452 $\mu$m HF channel for the water vapor retrieval (Ellis E. Remsberg, private communication, 2009). These revisions will probably result in an increase in water vapor mixing ratios in the tropical lower stratosphere. Further discussion will be presented in section 3.3.

[15] The MLS instrument utilizes thermal microwave to far infrared emission from the atmospheric limb to measure water vapor and other key constituents in the middle atmosphere including the upper troposphere [*Waters et al.*, 2006]. The measurements started in August 2004. The number of measurements in the latitudes 10°N–10°S within a month is 35,000–45,000 except for the first two months during which time the number was 25,000–35,000 per month. In this paper, MLS data version 2.2 are used (downloaded from http://mls.jpl.nasa.gov/ between May and August 2009). *Lambert et al.* [2007] estimated the precision of the version 2.2 water vapor data set as 4%–9% in the stratosphere and the accuracy as 4%–11% at 68–0.01 hPa. *Vömel et al.* [2007a] validated water vapor data from both versions 1.5 and 2.2 using coincident CFH measurements at 10 sites located between 67°N and 21°S between February 2005 and January 2007, sampling the fine-resolution CFH profiles with the smoothing function and averaging kernel of the MLS. It was found that the MLS data version 2.2 and CFH measurements agree on average to within 2.7% ± 8.7% between 68 hPa and 21.5 hPa.

## 3. Results and Discussion

### 3.1. Seasonal Variations

[16] Figure 3 shows water vapor profiles taken at Costa Rica arranged for four seasons. We observe that the profiles show distinct characteristics for each season. For example, in DJF there are two minima at ~80 hPa and at ~30 hPa and one maximum at ~50 hPa, while in JJA, there is only one minimum at ~60 hPa. This is the so-called tape recorder

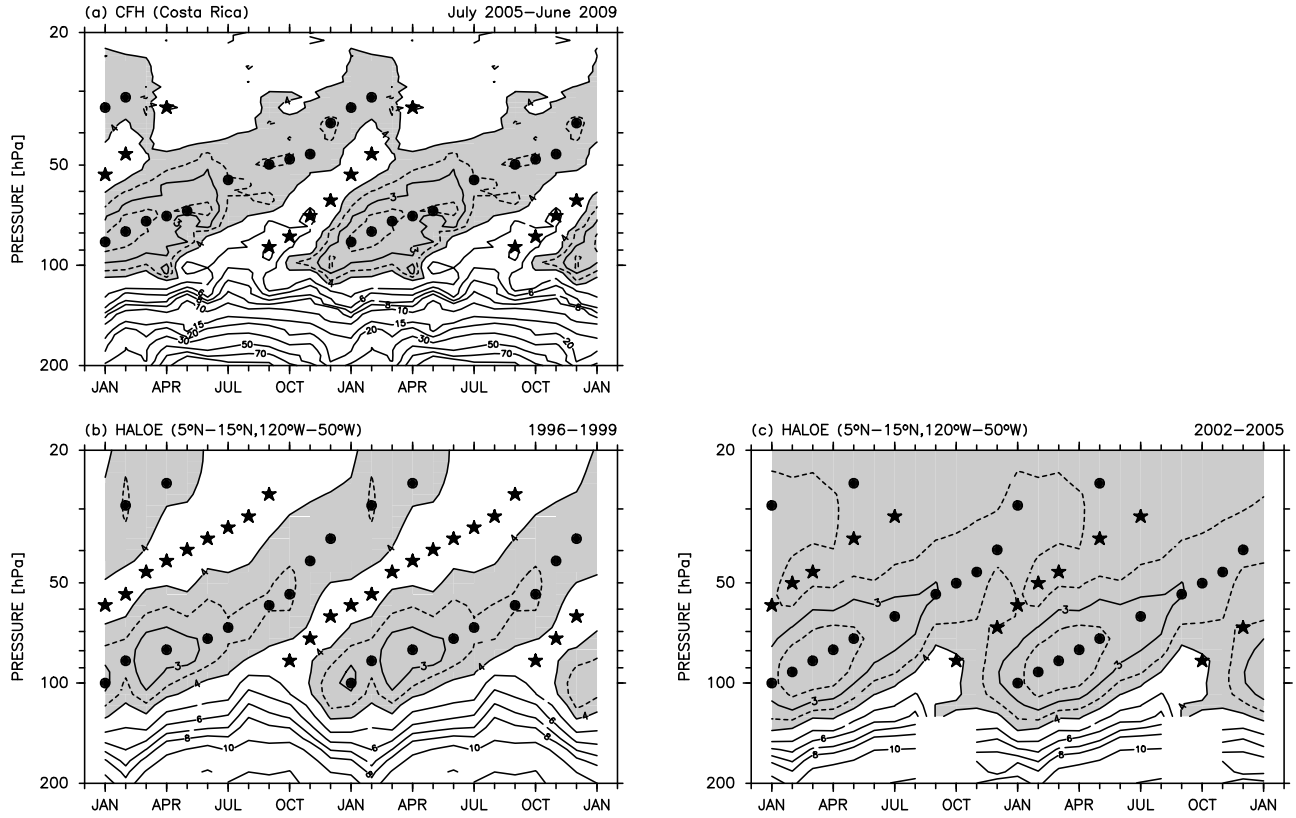


**Figure 4.** Climatological month-pressure distribution of water vapor mixing ratio (a) at Costa Rica over the period July 2005–June 2009 using CFH data, (b) in the Costa Rica region (5°N–15°N and 120°W–50°W) over the period 1996–1999 using HALOE data, and (c) as in Figure 4b, but for the period 2002–2005. Note that the annual cycle is repeated in order to gain a better sense of the tape recorder signal. The regions with ≤4 ppmv are colored gray. Mixing ratio numbers for the solid contours are shown. Dotted contours are for 2.5 and 3.5 ppmv. Circles and stars indicate the location of the minimum and maximum mixing ratios, respectively (see text).

signal. The seasonal cycle of water vapor is due to the seasonal cycle of tropical tropopause temperature (showing a minimum in northern winter and a maximum in northern summer), that is, the tropical tropopause acts as a tape head recording the water vapor mixing ratio. It should be noted that the mixing ratios below the top of the TTL (e.g., 70 hPa by *Fueglistaler et al.* [2009]) largely reflect the local/regional processes (around Costa Rica in this case) while those above this level represent the zonal mean concentrations; the effective entry value is determined by horizontal transport/mixing and dehydration processes within the TTL. The air is then transported upward associated with the Brewer-Dobson circulation, with its water vapor mixing ratio basically maintained. The signal is somewhat degraded by vertical diffusion and by dilution with midlatitude air [*Mote et al.*, 1998]. The contributions of production through the methane oxidation are small (up to ~10%) in the height region shown in this figure (see, e.g., *Randel et al.* [1998] for the vertical gradients of methane in the tropical lower stratosphere).

[17] In Figure 4, we show the CFH data from Costa Rica binned into monthly averages over the 4 years of the record. Before taking monthly averages, each profile has been averaged for over data bins with 250 m intervals. Note also that for determination of the minimum and maximum mixing ratio locations, we assumed that they always ascend with time. We observe a clear upward propagation of drier (wetter) air starting at the tropopause in northern winter (summer). Figure 4 also shows the month-pressure distribution of monthly averaged HALOE profiles around Costa Rica (5°N–15°N and 120°W–50°W) during the late 1990s and during the early 2000s. The difference in the mixing ratio in the stratosphere between the two periods will be discussed in section 3.3. The location of the tropopause minimum, at ~80 hPa in February for CFHs and at ~80 hPa in March for HALOE, is almost the same between the CFH and HALOE measurements.

[18] We use the ascent rate of the extrema in Figure 4 to roughly estimate the vertical velocity in the tropical lower stratosphere. Using the observed tape recorder signal, *Mote et al.* [1998] have estimated the vertical profiles of the "true" vertical velocity, vertical diffusion, and dilution by midlatitude air at the same time using a one-dimensional advection-diffusion-dilution equation, while *Niwano et al.* [2003] and *Schoeberl et al.* [2008] estimated only the vertical velocity, assuming that the vertical diffusion and dilution by midlatitude air are negligible. Here we focus on the ascent rate of only the extrema with the assumption in the latter two studies; the estimated vertical velocity may be the upper bound of the "true" vertical velocity because

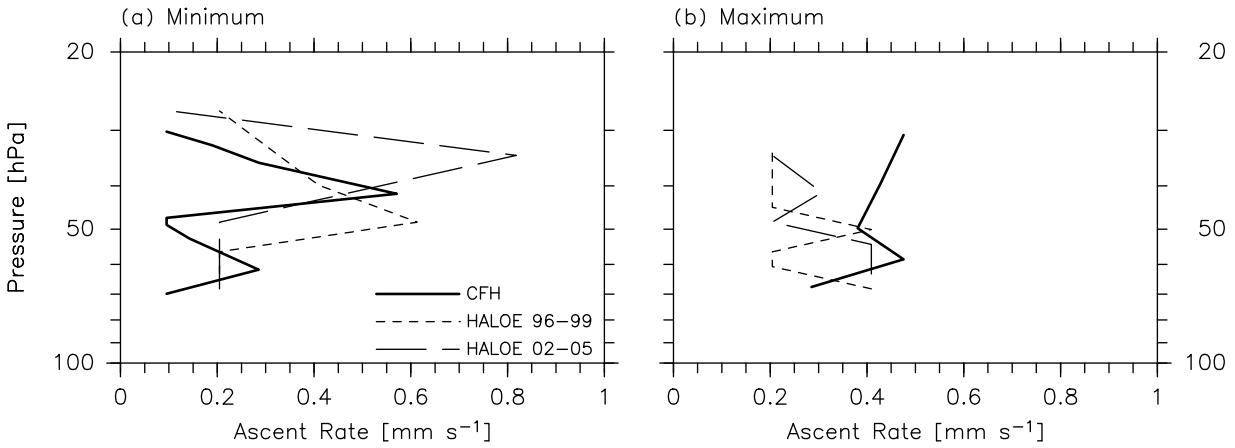


**Figure 5.** Ascent rate profiles calculated from (a) the minimum mixing ratio locations and (b) the maximum mixing ratio locations, using Costa Rica CFH data (solid), HALOE 1996–1999 data (dotted), and HALOE 2002–2005 data (dashed) shown in Figure 4.

vertical diffusion tends to accelerate the ascending tape recorder signal [e.g., *Schoeberl et al.*, 2008]. Figure 5 shows the ascent rate profiles for the minima and the maxima in Figure 4. The results for the CFH and HALOE measurements are similar. Except for the mixing-ratio minimum at 50–30 hPa, the ascent rate is 0.2–0.4 mm s$^{-1}$, which generally agrees with the previous studies. The minimum ascends faster (0.4–0.8 mm s$^{-1}$) at 50–30 hPa partly because it is in northern winter when the Brewer-Dobson circulation becomes stronger and probably partly because of the effect of vertical diffusion around this level. Note that the uncertainty of the ascent rate for the CFH measurements is estimated as ~0.05 mm s$^{-1}$ at 50 hPa if we assume that the major factor of the uncertainty is the uncertainty in radiosonde pressure measurements (0.5 hPa). For the HALOE measurements, the uncertainty is ~0.1 mm s$^{-1}$ if we take the reference pressure uncertainty of 2.3% [*Russell et al.*, 1993].

[19] Finally, we notice a clear difference between the CFH and HALOE measurements (Figure 4), that is, the vertical gradient of water vapor mixing ratio in the upper troposphere and even in the lower stratosphere. Figure 6 shows monthly averaged profiles in January and July. In particular, the positive vertical gradients at 80–60 hPa in January are much larger in the CFH measurements than in the HALOE measurements (see also Figure 12.) This might imply that the vertical diffusion and dilution by midlatitude air in this height region in this season might be overestimated using HALOE data [*Mote et al.*, 1998].

### 3.2. QBO Variations

[20] Figure 7 shows average profiles from the five SOWER campaigns in the tropical western Pacific in northern winter when CFHs were flown. Data from the subtropical station Ha Noi are excluded. We observe that the profiles in the December 2004, January 2007, and January 2009 campaigns (in bluish colors) are displaced downward from the profiles in the January 2006 and January 2008 campaigns (in reddish colors), with a geopotential height difference of ~1.5 km at 50–60 hPa. The QBO phase in the tropical lower stratosphere was a westerly phase for the former lower profiles, and an easterly phase for the latter higher profiles, as also shown in Figure 7. Figure 8 shows average profiles

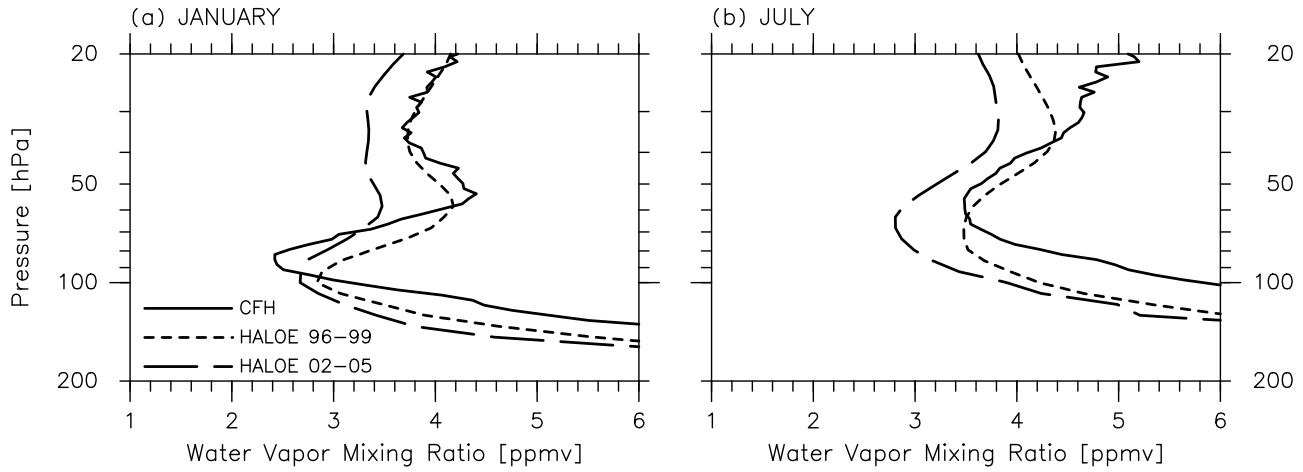


**Figure 6.** Monthly averaged profiles of water vapor mixing ratio at or near Costa Rica in (a) January and (b) July, shown in Figure 4. Solid curves are for Costa Rica CFH data, dotted curves are for HALOE 1996–1999 data, and dashed curves are for HALOE 2002–2005 data.

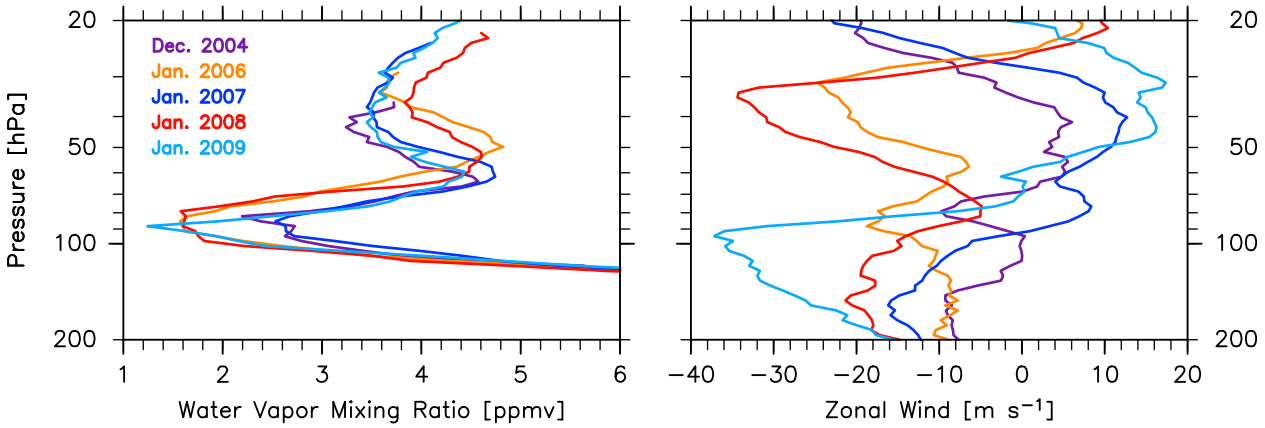


**Figure 7.** Average profiles of (left) water vapor mixing ratio and (right) zonal wind at equatorial western Pacific stations (i.e., Kototabang, Bandung, Biak, and Tarawa) during the five SOWER campaigns in December 2004 (purple), January 2006 (dark yellow), January 2007 (dark blue), January 2008 (red), and January 2009 (light blue).

at Costa Rica (10°N) from the three Ticosonde campaigns in northern summer. Above the 50 hPa level, it is clear that the vertical gradients of water vapor for July–August 2006 (in bluish colors) are greater than those for July–August 2005 and 2007 (in reddish colors), suggesting downward displacements for the former in this altitude region. The vertical displacement around 40–80 hPa may be estimated as ~1 km in geopotential height. The QBO phase in July–August 2006 was a weak easterly phase centered around 60 hPa, and the phase in July–August 2005 and 2007 was an easterly phase above the 50 hPa level.

[21] These vertical displacements are associated with the QBO meridional circulation anomalies [e.g., *Baldwin et al.*, 2001]. On the QBO time scales, the adiabatic temperature change associated with vertical motion in the thermodynamic equation is roughly balanced with the diabatic heating that can be approximated by a Newtonian cooling expression as

$$w\frac{HN^2}{R} \simeq -\alpha\delta T, \qquad (1)$$

where $w$ is vertical wind, $H$ is the scale height of the atmosphere, $N$ is the buoyancy frequency, $R$ is the gas constant for dry air, $\alpha$ is the Newtonian cooling coefficient, and $\delta T$ is the temperature anomaly. Therefore $w$ is roughly out of phase with $\delta T$, and the vertical displacement $\delta z$ is about a quarter cycle delayed from $w$. Figure 9 shows the zonal and monthly mean deseasonalized temperature anomaly and the vertical displacement obtained by integrating $w$ in equation (1) at the equator at 30, 50, and 70 hPa using European Centre for Medium-Range Weather Forecasts (ECMWF) reanalysis (ERA-Interim) temperature data. In the integration, $N$ was set to be $2.2 \times 10^{-1}$ s$^{-1}$ at all pressure levels. $\alpha$ is often taken as $5 \times 10^{-7}$ s$^{-1}$ (corresponding to a radiative damping time of ~20 days) in the lower stratosphere [*Baldwin et al.*, 2001], but *Niwano et al.* [2003] discussed that $\alpha$ may be smaller, e.g., $1 \times 10^{-7}$ s$^{-1}$ (100 days) around 70 hPa in the tropics. Thus Figure 9 shows $\delta z$ for both $\alpha = 5 \times 10^{-7}$s$^{-1}$ and $1 \times 10^{-7}$ s$^{-1}$ to show an uncertainty range. We observe that the sign of $\delta z$ corresponds to the sign of vertical displacement (either upward or downward) for the SOWER northern winter campaigns (Figure 7). For the Ticosonde northern summer campaigns (Figure 8), the signs agree at 30 hPa but may not agree well at lower levels; the QBO phases were not

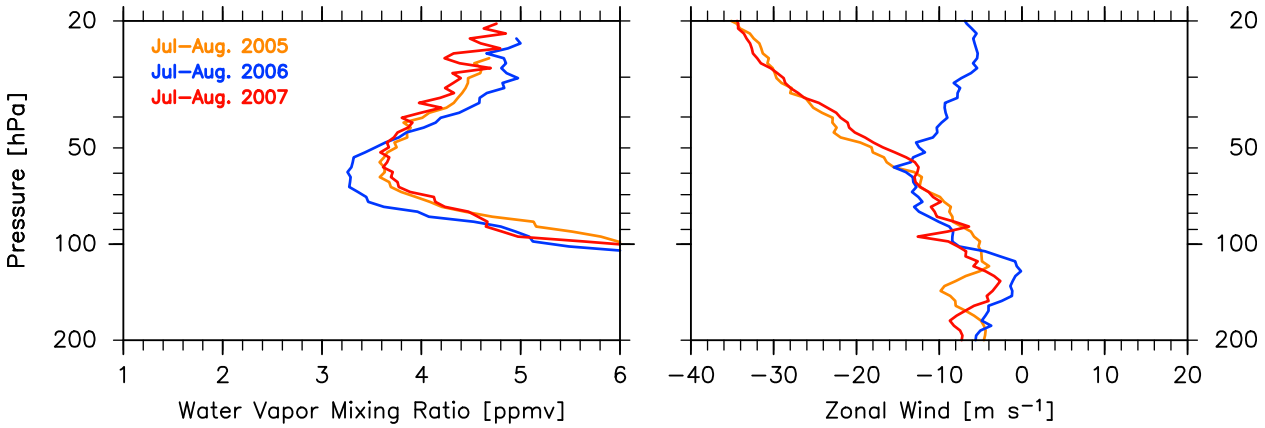


**Figure 8.** As for Figure 7, but for Costa Rica during the three Ticosonde campaigns in July–August 2005 (dark yellow), July–August 2006 (dark blue), and July–August 2007 (red).

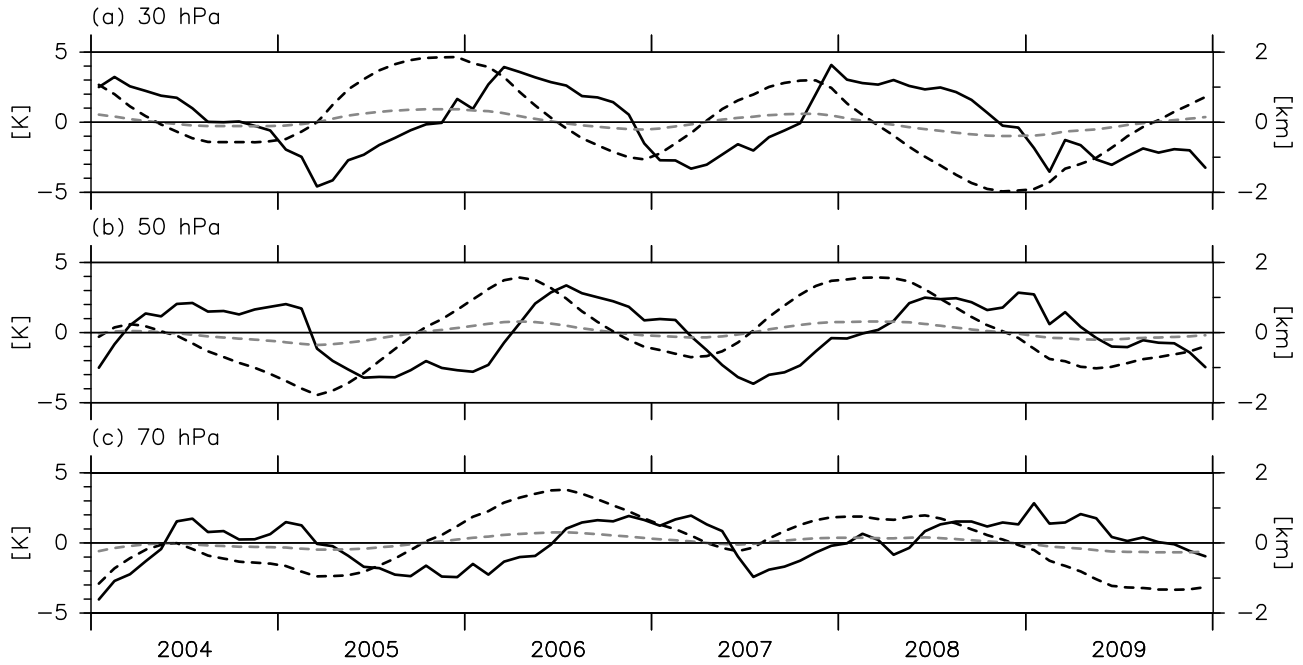


**Figure 9.** Time series of zonal and monthly mean equatorial temperature anomaly deseasonalized with respect to the 2004–2009 climatology (solid; in Kelvin) and the estimated vertical displacement (dotted black for $\alpha = 5 \times 10^{-7}$ s$^{-1}$ and dotted gray for $\alpha = 1 \times 10^{-7}$ s$^{-1}$; in km; see text for details) at (a) 30 hPa, (b) 50 hPa, and (c) 70 hPa.

ideal for these campaigns to look at the QBO meridional circulation anomaly effect in the vertical profiles. Also, the amplitude of $\delta z$ (<2 km) shown in Figure 9 broadly agrees with the results in Figures 7 and 8 (note that the vertical displacements shown in these figures may show the twice of the amplitude).

[22] We observe another effect of the QBO on the water vapor in the tropical lower stratosphere in Figures 7 and 8. Figure 7 shows that the minimum at 80–100 hPa (representing the concentration in the western Pacific region) and the secondary minimum at 30–40 hPa (representing the concentration in the global tropics) both indicate a variation with roughly a 2 year periodicity. The difference in concentration is ~0.5 ppmv. The two minima are connected qualitatively such that higher (lower) concentrations at 30–40 hPa are the result of higher (lower) concentrations at 80–100 hPa in the previous winter. Note that the tropopause region over the tropical western Pacific is coldest throughout the year and thus largely controls the entry value of water vapor [*Holton and Gettelman*, 2001]. Figure 8 also shows that the minimum at 50–70 hPa (reflecting the concentration in the global tropics) indicates a two-year periodicity with a ~0.5 ppmv difference and that its concentrations qualitatively reflect the concentrations at 80–100 hPa in the tropical western Pacific in the previous winter shown in Figure 7. It should be noted that we also observe the QBO variability in saturation water vapor mixing ratio at 100 hPa over the tropical western Pacific using reanalysis data sets (see Figure 13). The QBO-related mixing ratio anomalies created at the tropical tropopause propagate upward by the Brewer-Dobson circulation. Note also that the observed ~0.5 ppmv changes due to the QBO are consistent with the estimation by *Fueglistaler and Haynes* [2005] who used ECMWF 40 year reanalysis (ERA40) temperature and wind data [*Uppala et al.*, 2005] at the 400 K potential temperature level.

[23] Figure 10 shows average profiles at Ha Noi (21.01°N) from the three SOWER campaigns in northern winter. We observe that the secondary minimum at 30–40 hPa shows a weak biennial oscillation: The concentration in January 2008 is larger than that in January 2007 and in January 2009. This is qualitatively consistent with the variation at the same level over the equatorial western Pacific as shown in Figure 7. However, the zonal wind profiles indicate that the site is primarily affected by the midlatitude westerly jet centered around 200 hPa, and as shown by *Randel et al.* [1999], the QBO signals in zonal wind becomes almost zero in this latitude region. Nevertheless, there seems to exist a link in the water vapor field at this level between the equatorial region and this latitude region, probably through horizontal transport/mixing, on the QBO time scale. The concentration at the lower minimum at 80–100 hPa is primarily controlled by the air flow around this level on subseasonal time scales. When air comes from the equatorial western Pacific, the concentration tends to be lower.

### 3.3. Decadal Variations

[24] Figure 11 shows the time series of water vapor mixing ratio averaged for 68–37 hPa (corresponding roughly to 19–23 km) using NOAA FPH, CFH, and satellite 10°N–10°S data. For NOAA FPH and SOWER CFH data, campaign averages are shown. For Ticosonde CFH and satellite data, monthly averages are shown. Note that lower quality HALOE data (particularly before mid-1992) are not plotted. As shown in Tables 1 and 2 and in Figure 2, only the NOAA FPH and CFH profiles with good quality data

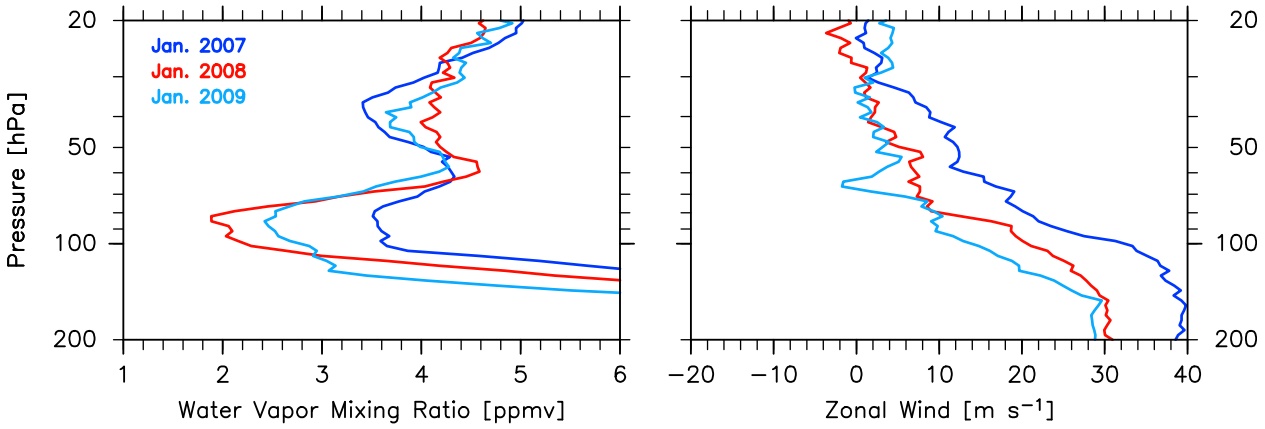


**Figure 10.** As for Figure 7, but for Ha Noi during the three SOWER campaigns in January 2007 (dark blue), January 2008 (red), and January 2009 (light blue).

points above the 37 hPa level are used in Figure 2. The reason for the choice of layer between 68 hPa and 37 hPa is explained below. The water vapor concentrations around the tropopause region strongly reflect the local temperature variations on subseasonal time scales. As noted in section 3.1, the upper boundary of the TTL is often considered to be 70 hPa [e.g., *Fueglistaler et al.*, 2009] as above this level lower stratospheric characteristics dominate, and thus local measurements largely reflect the zonal mean field. In the tropical lower stratosphere there is a clear seasonal cycle in the water vapor profile, i.e., the tape recorder signal. Therefore taking a certain layer average would be appropriate to investigate interannual variability. For NOAA FPH and CFH data, the upper bound of good quality data depends on each sounding, and successful soundings reaching the 30 hPa level are relatively few. For satellite data, the number of data levels are limited. Considering these factors, we chose the 68–37 hPa layer. The HALOE data version 19 with the file version P1.6 used here has 9 levels between 68 hPa and 37 hPa, and the MLS data version 2.2 used here has 4 levels between 68 hPa and 38 hPa. Note that the vertical bars show the standard error of the mean, which is the standard deviation divided by a square root of the number of (independent) measurements. For CFH data, we assumed conservatively that the measurements are independent for every ~250 m. As described in section 2.1, the NOAA FPH data taken in the CEPEX campaign were adjusted to the HALOE measurements [*Vömel et al.*, 1995a].

[25] Figure 11 shows that there are three distinct periods, the 1990s, the early 2000s, and the mid to late 2000s. In the

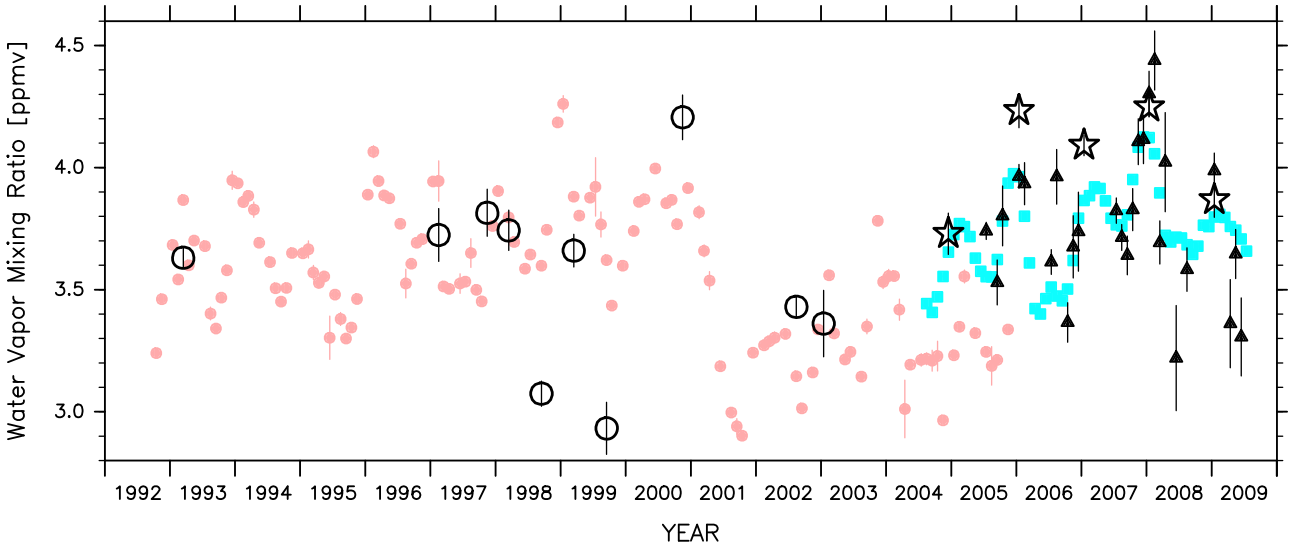


**Figure 11.** Time series of water vapor mixing ratio averaged for 68–37 hPa using NOAA FPH and CFH (except for Ha Noi) data and 10°N–10°S HALOE and MLS data. Open circles indicate NOAA FPH campaign averages, and open stars indicate SOWER CFH campaign averages. Closed triangles indicate Ticosonde CFH monthly averages. Closed circles colored pink indicate HALOE monthly averages (sunrise and sunset data are mixed), and closed squares colored light blue indicate MLS monthly averages. Vertical bars show the standard error of the mean (see text for details). For satellite data, the bars are generally smaller than the symbols in size.

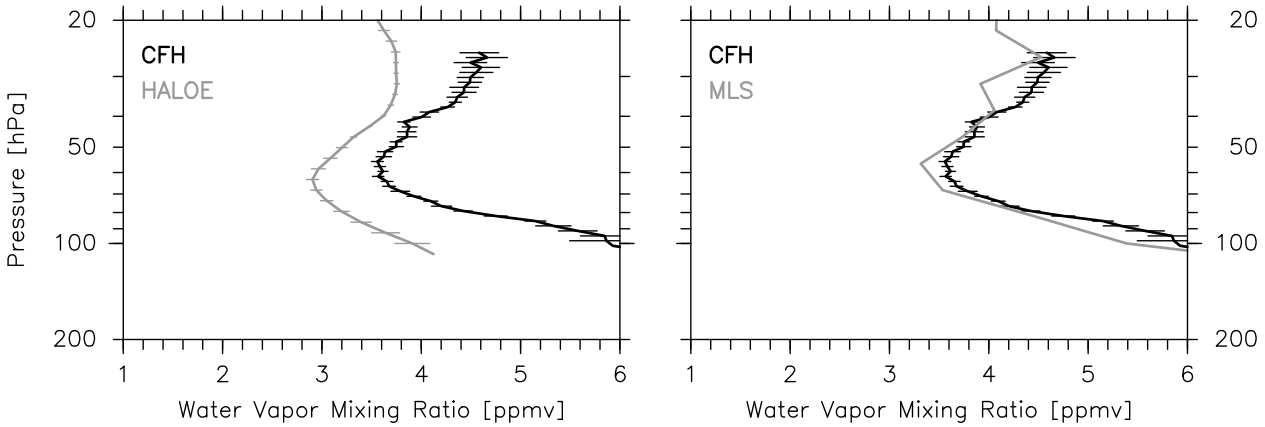


**Figure 12.** Average profiles of water vapor mixing ratio from (a) 13 CFH measurements at Costa Rica (black) and 5 HALOE profiles around Costa Rica (gray) and (b) the same CFH measurements as in Figure 12a (black) and 1189 MLS profiles around Costa Rica (gray), during July 2005. Horizontal bars indicate the standard error of the mean. For MLS data, the bars are smaller than the thickness of the curve.

1990s, both HALOE and NOAA FPH data generally indicate a gradual increase that has been reported previously [e.g., *Rosenlof et al.*, 2001]. The HALOE averages for 1993–1996 and for 1997–2000 are 3.64 and 3.78 ppmv, respectively. The two exceptionally low NOAA FPH values are taken in September 1998 and in September 1999 both at San Cristóbal Island and might be in part due to small sampling numbers. In the early 2000s, the concentrations are low after the drop around 2000–2001 as clearly indicated with HALOE data. The HALOE average for 2001–2004 is 3.29 ppmv. The three NOAA FPH campaigns between late 2000 and early 2003 support the occurrence of this drop. After 2004, the concentrations might have become ~0.5 ppmv higher than those in the early 2000s. The Costa Rica CFH average for July 2005–June 2009 is 3.77 ppmv, and the MLS average for 2005–2008 is 3.74 ppmv. (Note that the standard error of the mean for the above 4 year averages is quite small, i.e. 0.01 ppmv for CFH and 0.001 ppmv for HALOE and MLS.) However, as will be discussed in the next paragraph, the HALOE measurements may have a dry bias of ~0.3 ppmv or larger, and thus the changes from the early 2000s to the late 2000s may be smaller. Note that the CFH and MLS measurements show similar variations also on seasonal and QBO time scales. (The components on these time scales remain even after the layer averaging.)

[26] A closer look at Figure 11 around 2004–2005 suggests that the HALOE measurements may be ~0.3 ppmv lower than the CFH and MLS measurements. (*Lambert et al.* [2007] have already reported that there are similar biases between the MLS and HALOE measurements in the global stratosphere.) In July 2005, there were 13 CFH soundings at Costa Rica that reached the 100 hPa level and above (note that Figure 2 may show only 11 soundings, but there were actually two soundings on 22 and on 24 July 2005). During this period, the HALOE data set has 5 profiles and the MLS has 1189 profiles in the region around Costa Rica, 5°N–15°N and 120°W–50°W. Figure 12 shows intercomparisons of the HALOE, MLS, and CFH measurements around Costa Rica in July 2005. Note that the averaging kernel of the satellite measurements is not considered here. But, as described in section 2.2, *Vömel et al.* [2007a] have shown that the MLS data version 2.2 and CFH data degraded with the MLS averaging kernel agree on average to within 2.7% ± 8.7% between 68 hPa and 21.5 hPa. Figure 12 shows that the HALOE and CFH measurements are consistently biased throughout the tropical lower stratosphere (e.g., ~0.4 ppmv around 50 hPa and ~1 ppmv at 80 hPa), while the difference between the MLS and CFH measurements is small (<~0.2 ppmv around 60 hPa). Therefore CFH and MLS data suggest that the HALOE measurements have a dry bias in the tropical lower stratosphere (~0.4–1 ppmv in July 2005 over Costa Rica and ~0.3 ppmv on average at least over the period 2004–2005). Also, *Wrotny et al.* [2010] compared water vapor data from the Atmospheric Chemistry Experiment-Fourier Transform Spectrometer (ACE-FTS) on board the SCISAT-1 satellite and from HALOE for February and August of 2004 and 2005 at 10°N–10°S and showed that HALOE water vapor is ~10% lower than ACE-FTS water vapor at 100–20 hPa. (Note that *Lambert et al.* [2007] showed very good agreement between the MLS and ACE-FTS measurements.) As described in section 2.2, the HALOE team is currently preparing the data version 20 which may give somewhat higher water vapor mixing ratios in the tropical lower stratosphere.

[27] In summary, water vapor mixing ratios were higher and increasing in the 1990s, lower in the early 2000s, and probably slightly higher again or recovering after 2004. These facts suggest the existence of decadal variations in tropical lower stratospheric water vapor [e.g., *Solomon et al.*, 2010], not simply upward trends and the drop discussed previously.

[28] Finally, we investigate interannual variations of the water vapor entry value using five reanalysis temperature data sets that are independent of the water vapor measurements. Figure 13 shows time series of 1 year running averaged saturation water vapor mixing ratio at 100 hPa in the tropical western Pacific cold region, a proxy for the entry value, calculated from temperature data in the five reanalyses which are ERA40, the more recent ECMWF reanalysis (ERA-Interim), the Japanese reanalysis (JRA25/JCDAS)

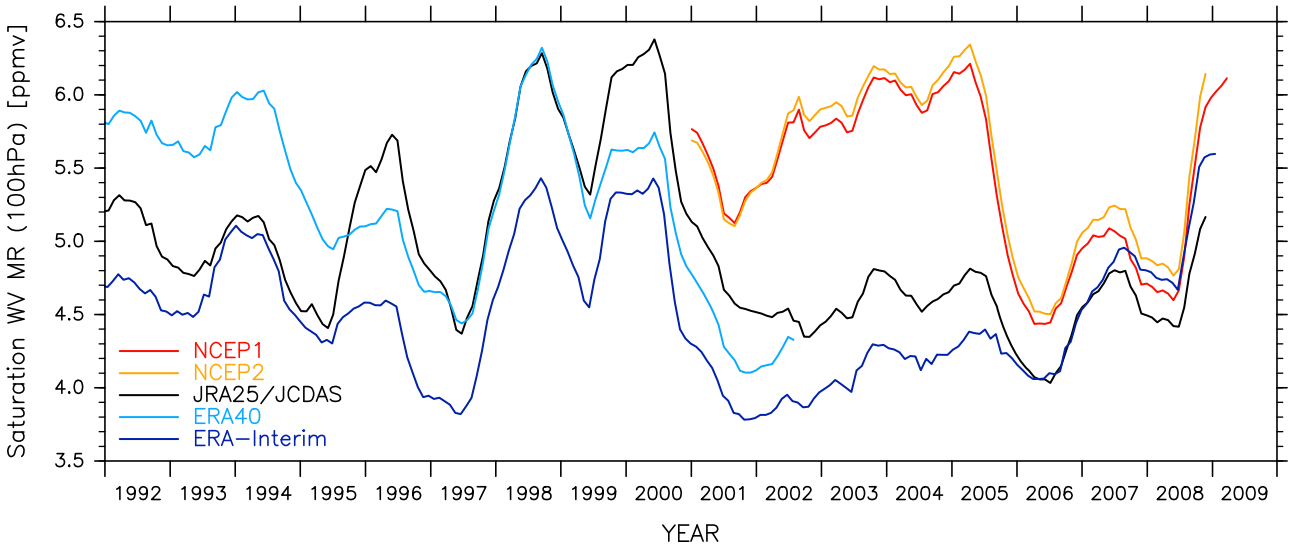


**Figure 13.** Time series of 1 year running averaged saturation water vapor mixing ratio at 100 hPa in the tropical western Pacific (10°N–10°S and 120°E–150°W) calculated from temperature data from NCEP1 (red), NCEP2 (dark yellow), JRA25/JCDAS (black), ERA40 (light blue), and ERA-Interim (dark blue) reanalysis. The 1 year running averages are taken between -365 day and 0 day at a given time. Note that NCEP1 and NCEP2 data are shown only after 2001. See text for details.

[*Onogi et al.*, 2007], the NCEP/NCAR reanalysis data (NCEP1) [*Kalnay et al.*, 1996], and the NCEP-DEO AMIP-II reanalysis data (NCEP2) [*Kanamitsu et al.*, 2002]. The Goff 1965 formulation presented by *Murphy and Koop* [2005] is used for the conversion of temperature to saturation water vapor partial pressure. The tropical western Pacific region (10°N–10°S and 120°E–150°W) is chosen because the tropopause over this region is considered to largely determine the entry value of water vapor [*Holton and Gettelman*, 2001]. However, the following discussion does not change qualitatively if we choose, e.g., the global tropics (10°N–10°S) [see also *Fueglistaler and Haynes*, 2005].

[29] Figure 13 shows that ERA40, ERA-Interim, and JRA25/JCDAS data indicate general agreement particularly for interannual variability from the QBO to decadal time scales. These three data sets show a large drop around 2000–2001 (1.5–2 ppmv, corresponding to a temperature drop of ~2 K) and a gradual recovery through the 2000s; this is qualitatively consistent with the water vapor observations shown in Figure 11. It should be noted that NCEP1 and NCEP2 100 hPa temperature data show strong negative trends in the 1990s and that the corresponding saturation water vapor mixing ratios in the beginning of the 1990s are as high as nearly 10 ppmv; thus NCEP1 and NCEP2 data are shown only after 2001 in Figure 13 (*Randel et al.* [2002] showed that NCEP1 data have 2–3 K warm biases at the tropical tropopause). Also, note that there is a constant offset in Figure 13 (even for ERA40, ERA-Interim, and JRA25/JCDAS) with respect to Figure 11; this is probably due to the fact that 100 hPa temperatures are generally greater than the cold-point temperatures, and that the averaging procedures have smoothed out subseasonal variability in tropopause temperatures associated with, for example, equatorial Kelvin waves. Also, the region of 10°N–10°S and 120°E–150°W may be too wide to specify the primary dehydration region. Figure 13 (except for NCEP1 and NCEP2 data) supports the existence of decadal variations in the tropical lower stratospheric water vapor.

[30] The decadal changes around the tropical tropopause over the tropical western Pacific, which have caused the decadal variations of water vapor in the tropical lower stratosphere, may have been resulted from changes in the Brewer-Dobson circulation [*Randel et al.*, 2006] or from changes in the sea surface temperatures and convective activity in the western Pacific [*Rosenlof and Reid*, 2008] or from both. The 11 year solar cycle and major volcanic eruptions could also have some contributions. However, *Yamashita et al.* [2010] estimated the solar cycle contribution as only 0.2 K in the tropical lower stratosphere using a chemistry climate model. Also, there was no major volcanic eruption that directly affected the global stratosphere after 1994. We note that the characteristics of the ENSO may be different before and after the 1997–1998 record strong warm event (El Niño event). Before this event, warm events occurred every 3–7 years, while after this event, cold events (La Niña events) occurred for three subsequent years (i.e., 1998–1999, 1999–2000, and 2000–2001) and then warm events occurred roughly every 2 years (i.e., 2002, 2004–2005, 2006). (The ENSO phases here are determined from the Southern Oscillation Index prepared by NOAA.) The colder tropopause temperatures in the early 2000s might be related with these ENSO characteristics. It should also be pointed out that when not subjected to a running average, the time series of ERA-Interim 100 hPa temperature for the tropical western Pacific (not shown) indicate that not only the northern winter minimum was low particularly in 2000–2001 and in 2001–2002 but also the northern summer maximum was low in 2001 and in 2002 and relatively low in 2000 and in 2003. Therefore northern summer processes as well as northern winter processes may be important to

explain the decadal variations of tropopause temperatures in the tropical western Pacific and water vapor mixing ratios in the global lower stratosphere.

## 4. Conclusions

[31] We investigated water vapor variations in the tropical lower stratosphere on seasonal, QBO, and decadal time scales using in situ, balloon-borne cryogenic frost point hygrometer (NOAA FPH and CFH) data taken at various tropical sites over the last 17 years, 1993–2009. Data from the UARS HALOE (1991–2005) and EOS Aura MLS (2004–2009) and from reanalyses were also analyzed and compared with the in situ water vapor data. Because water vapor variations on these time scales had been investigated extensively with HALOE data, the emphasis was also on the quantitative comparisons between HALOE and our in situ data.

[32] Quasi-regular CFH sounding data taken at Costa Rica between July 2005 and June 2009 clearly showed the tape recorder signal. The ascent rates calculated from the minimum and maximum water vapor mixing ratios using monthly averaged CFH data agree well with those using HALOE data for 1996–1999 and for 2002–2005. A clear difference between CFHs and HALOE is the vertical gradient in the lower stratosphere, particularly in northern winter at 80–60 hPa. This has an implication for the vertical diffusion and dilution by midlatitude air which were previously estimated with HALOE data.

[33] Average profiles from the five SOWER CFH campaigns in the equatorial western Pacific in northern winter and from the three Ticosonde CFH campaigns at Costa Rica (10°N) in northern summer clearly showed two effects of the QBO. One is the vertical displacement of water vapor profiles (the maximum-to-minimum difference of 1–1.5 km) in association with the QBO meridional circulation anomalies. We found that the thermodynamic balance between the adiabatic temperature change and the diabatic heating [e.g., *Baldwin et al.*, 2001] reasonably explains the observed vertical displacement of water vapor profiles. The other is the concentration variations (the maximum-to-minimum difference of ~0.5 ppmv) in association with the QBO tropopause temperature variations. The QBO-related mixing ratio anomalies created at the tropical tropopause propagate upward by the Brewer-Dobson circulation. At Ha Noi (21°N), there is a weak link to the equatorial region through horizontal transport/mixing on subseasonal time scales around the tropopause and on the QBO time scale in the lower stratosphere.

[34] Time series of all tropical NOAA FPH and CFH data averaged in a lower stratospheric layer (68–37 hPa) together with HALOE and MLS data showed the existence of decadal variations in tropical lower stratospheric water vapor, not simply upward trends and the drop around 2000–2001. In the 1990s, both HALOE and NOAA FPH data generally indicate a gradual increase that has been reported previously. In the early 2000s, the concentrations are low after the drop around 2000–2001. After 2004, the concentrations may become slightly higher than those in the early 2000s and may show an increase again. It should be noted that we found that the HALOE measurements may have a dry bias of ~0.3 ppmv or larger compared with the CFH and MLS measurements in the tropical lower stratosphere at least during 2004–2005. Thus the changes between the early 2000s (measured primarily with the HALOE) and the late 2000s (measured with the CFH and MLS) may be smaller than those indicated by the original measurements. The observed decadal changes in lower stratospheric water vapor are generally in good agreement with 100 hPa temperature data in the tropical western Pacific from the ERA40, ERA-Interim, and JRA25/JCDAS reanalyses. The decadal variations in the tropical tropopause temperature and in the tropical lower stratospheric water vapor during the past ~20 years may have been caused by changes in the stratospheric circulation [*Randel et al.*, 2006] and/or the sea surface temperature with similar time scales [*Rosenlof and Reid*, 2008; *Solomon et al.*, 2010], but further studies are necessary.

[35] Water vapor in the lower stratosphere has important roles in the global atmospheric chemistry and climate through its radiative and photochemical nature. Long-term, accurate measurements using in situ, cryogenic frost point hygrometers are thus crucial to monitor one of the important factors of our climate system.

[36] **Acknowledgments.** The balloon-borne water vapor measurements presented in this paper have been conducted with strong, long-term support from the Instituto Nacionál de Meteorología e Hidrología (INAMHI), Ecuador, the Indonesian National Institute of Aeronautics and Space (LAPAN), Indonesia, the National Hydro-Meteorological Service, Ministry of Natural Resources and Environment, Vietnam, the Kiribati Meteorological Service, Kiribati, and Universidad Nacional, Costa Rica. The SOWER project has been financially supported by the Sumitomo Foundation, the Asahi Breweries Foundation, the Japanese Ministry of Education, Culture, Sports, Science and Technology (MEXT) through Grants-in-Aid for Scientific Research (10041103, 11219201, 15204043, 18204041, and 19740283), the Ministry of the Environment through the Global Environment Research Fund (A-1 and A-071), and RISH, Kyoto University. Support for the sounding program in Costa Rica has been provided by the NASA Upper Atmosphere Research Program, the Radiation Sciences Program, and the Aura Satellite Project. The HALOE data were provided by GATS, Inc., through their Web site. The EOS Aura MLS data were provided by the NASA/JPL through their Web site. The ERA40 and ERA-Interim data were provided by the ECMWF through their Web site (the ERA40 data were actually obtained through an authorized Web site at RISH, Kyoto University). The JRA25/JCDAS data were provided by the JMA and CRIEPI. The NCEP1 and NCEP2 reanalysis data were provided by the NOAA/OAR/ESRL PSD. We thank Takashi Imamura, Masanori Niwano, and Takatoshi Sakazaki for valuable discussion. We also thank Stephan Fueglistaler and two anonymous reviewers for valuable comments. All figures were produced using the GFD-DENNOU Library.

## References

Baldwin, M. P., et al. (2001), The quasi-biennial oscillation, *Rev. Geophys.*, *39*(2), 179–229.

Fueglistaler, S., and P. H. Haynes (2005), Control of interannual and long-term variability of stratospheric water vapor, *J. Geophys. Res.*, *110*, D24108, doi:10.1029/2005JD006019.

Fueglistaler, S., A. E. Dessler, T. J. Dunkerton, I. Folkins, Q. Fu, and P. W. Mote (2009), Tropical tropopause layer, *Rev. Geophys.*, *47*, RG1004, doi:10.1029/2008RG000267.

Fujiwara, M., F. Hasebe, M. Shiotani, N. Nishi, H. Vömel, and S. J. Oltmans (2001), Water vapor control at the tropopause by equatorial Kelvin waves observed over the Galápagos, *Geophys. Res. Lett.*, *28*(16), 3143–3146, doi:10.1029/2001GL013310.

Harries, J., J. Russell III, A. Tuck, L. Gordley, P. Purcell, K. Stone, R. Bevilacqua, M. Gunson, G. Nedoluha, and W. Traub (1996), Validation of measurements of water vapor from the Halogen Occultation Experiment (HALOE), *J. Geophys. Res.*, *101*(D6), 10,205–10,216, doi:10.1029/95JD02933.

Hasebe, F., M. Fujiwara, N. Nishi, M. Shiotani, H. Vömel, S. Oltmans, H. Takashima, S. Saraspriya, N. Komala, and Y. Inai (2007), In situ observations of dehydrated air parcels advected horizontally in the

tropical tropopause layer of the western Pacific, *Atmos. Chem. Phys.*, *7*, 803–813.

Holton, J. R., and A. Gettelman (2001), Horizontal transport and the dehydration of the stratosphere, *Geophys. Res. Lett.*, *28*(14), 2799–2802, doi:10.1029/2001GL013148.

Holton, J. R., P. Haynes, M. McIntyre, A. Douglass, R. Rood, and L. Pfister (1995), Stratosphere-troposphere exchange, *Rev. Geophys.*, *33*(4), 403–439.

Inai, Y. (2010), Cold trap dehydration in the tropical tropopause layer estimated from the water vapor match, Ph.D. dissertation, Grad. School of Environ. Sci., Hokkaido Univ., Sapporo, Japan.

Kalnay, E., et al. (1996), The NCEP/NCAR 40 year reanalysis project, *Bull. Am. Meteorol. Soc.*, *77*(3), 437–471.

Kanamitsu, M., W. Ebisuzaki, J. Woollen, S.-K. Yang, J. J. Hnilo, M. Fiorino, and G. L. Potter (2002), NCEP-DEO AMIP-II reanalysis (R-2), *Bull. Am. Meteorol. Soc.*, *83*(11), 1631–1643.

Kley, D., J. M. Russell, and C. Phillips (Eds.) (2000), SPARC assessment of upper tropospheric and stratospheric water vapour, *WCRP 113*, 312 pp., World Meteorol. Organ., Geneva, Switzerland.

Lambert, A., et al. (2007), Validation of the Aura Microwave Limb Sounder middle atmosphere water vapor and nitrous oxide measurements, *J. Geophys. Res.*, *112*, D24S36, doi:10.1029/2007JD008724.

Lanzante, J. R. (2009), Comment on "Trends in the temperature and water vapor content of the tropical lower stratosphere: Sea surface connection" by Karen H. Rosenlof and George C. Reid, *J. Geophys. Res.*, *114*, D12104, doi:10.1029/2008JD010542.

Mote, P., K. Rosenlof, M. McIntyre, E. Carr, J. Gille, J. Holton, J. Kinnersley, H. Pumphrey, J. Russell III, and J. Waters (1996), An atmospheric tape recorder: The imprint of tropical tropopause temperatures on stratospheric water vapor, *J. Geophys. Res.*, *101*(D2), 3989–4006, doi:10.1029/95JD03422.

Mote, P. W., T. J. Dunkerton, M. E. McIntyre, E. A. Ray, P. H. Haynes, and J. M. Russell III (1998), Vertical velocity, vertical diffusion, and dilution by midlatitude air in the tropical lower stratosphere, *J. Geophys. Res.*, *103*(D8), 8651–8666, doi:10.1029/98JD00203.

Murphy, D. M., and T. Koop (2005), Review of the vapour pressures of ice and supercooled water for atmospheric applications, *Q. J. R. Meteorol. Soc.*, *131*, 1539–1565.

Niwano, M., K. Yamazaki, and M. Shiotani (2003), Seasonal and QBO variations of ascent rate in the tropical lower stratosphere as inferred from UARS HALOE trace gas data, *J. Geophys. Res.*, *108*(D24), 4794, doi:10.1029/2003JD003871.

Oltmans, S., H. Vömel, D. Hofmann, K. Rosenlof, and D. Kley (2000), The increase in stratospheric water vapor from balloonborne, frostpoint hygrometer measurements at Washington, D. C., and Boulder, Colorado, *Geophys. Res. Lett.*, *27*(21), 3453–3456, doi:10.1029/2000GL012133.

Onogi, K., et al. (2007), The JRA-25 reanalysis, *J. Meteorol. Soc. Jpn.*, *85*(3), 369–432.

Peter, T., C. Marcolli, P. Spichtinger, T. Corti, M. B. Baker, and T. Koop (2006), When dry air is too humid, *Science*, *314*(5804), 1399–1402, doi:10.1126/science.1135199.

Randel, W. J., F. Wu, J. M. Russell III, A. Roche, and J. W. Waters (1998), Seasonal cycles and QBO variations in stratospheric $CH_4$ and $H_2O$ observed in UARS HALOE data, *J. Atmos. Sci.*, *55*(2), 163–185.

Randel, W. J., F. Wu, R. Swinbank, J. Nash, and A. O'Neill (1999), Global QBO circulation derived from UKMO stratospheric analyses, *J. Atmos. Sci.*, *56*(4), 457–474.

Randel, W. J., F. Wu, A. Gettelman, J. M. Russell III, J. M. Zawodny, and S. J. Oltmans (2001), Seasonal variation of water vapor in the lower stratosphere observed in Halogen Occultation Experiment data, *J. Geophys. Res.*, *106*(D13), 14,313–14,325.

Randel, W., M.-L. Chanin, and C. Michaut (Eds.) (2002), SPARC intercomparison of middle atmosphere climatologies, *WCRP 116*, 96 pp., World Meteorol. Organ., Geneva, Switzerland.

Randel, W. J., F. Wu, S. J. Oltmans, K. Rosenlof, and G. E. Nedoluha (2004), Interannual changes of stratospheric water vapor and correlations with tropical tropopause temperatures, *J. Atmos. Sci.*, *61*, 2133–2148.

Randel, W. J., F. Wu, H. Vömel, G. E. Nedoluha, and P. Forster (2006), Decreases in stratospheric water vapor after 2001: Links to changes in the tropical tropopause and the Brewer-Dobson circulation, *J. Geophys. Res.*, *111*, D12312, doi:10.1029/2005JD006744.

Rohs, S., C. Schiller, M. Riese, A. Engel, U. Schmidt, T. Wetter, I. Levin, T. Nakazawa, and S. Aoki (2006), Long-term changes of methane and hydrogen in the stratosphere in the period 1978–2003 and their impact on the abundance of stratospheric water vapor, *J. Geophys. Res.*, *111*, D14315, doi:10.1029/2005JD006877.

Rosenlof, K. H. (2002), Transport changes inferred from HALOE water and methane measurements, *J. Meteorol. Soc. Jpn.*, *80*(4B), 831–848.

Rosenlof, K. H., and G. C. Reid (2008), Trends in the temperature and water vapor content of the tropical lower stratosphere: Sea surface connection, *J. Geophys. Res.*, *113*, D06107, doi:10.1029/2007JD009109.

Rosenlof, K. H., and G. C. Reid (2009), Reply to comment by John R. Lanzante on "Trends in the temperature and water vapor content of the tropical lower stratosphere: Sea surface connection," *J. Geophys. Res.*, *114*, D12105, doi:10.1029/2008JD011265.

Rosenlof, K. H., et al. (2001), Stratospheric water vapor increases over the past half-century, *Geophys. Res. Lett.*, *28*(7), 1195–1198, doi:10.1029/2000GL012502.

Russell, J. M., III, L. L. Gordley, J. H. Park, S. R. Drayson, W. D. Hesketh, R. J. Cicerone, A. F. Tuck, J. E. Frederick, J. E. Harries, and P. J. Crutzen (1993), The Halogen Occultation Experiment, *J. Geophys. Res.*, *98*(D6), 10,777–10,797, doi:10.1029/93JD00799.

Scherer, M., H. Vömel, S. Fueglistaler, S. J. Oltmans, and J. Staehelin (2008), Trends and variability of midlatitude stratospheric water vapour deduced from the re-evaluated Boulder balloon series and HALOE, *Atmos. Chem. Phys.*, *8*, 1391–1402.

Schoeberl, M. R., A. R. Douglass, R. S. Stolarski, S. Pawson, S. E. Strahan, and W. Read (2008), Comparison of lower stratospheric tropical mean vertical velocities, *J. Geophys. Res.*, *113*, D24109, doi:10.1029/2008JD010221.

Seidel, D. J., et al. (2009), Reference upper-air observations for climate: Rationale, progress, and plans, *Bull. Am. Meteorol. Soc.*, *90*(3), 361–369.

Selkirk, H. B., H. Vömel, J. M. Valverde Canossa, L. Pfister, J. A. Diaz, W. Fernández, J. Amador, W. Stolz, and G. Peng (2010), Detailed structure of the tropical upper troposphere and lower stratosphere as revealed by balloonsonde observations of water vapor, ozone, temperature and winds during the NASA TCSP and TC4 campaigns, *J. Geophys. Res.*, doi:10.1029/2009JD013209, in press.

Sherwood, S. (2002), A microphysical connection among biomass burning, cumulus clouds, and stratospheric moisture, *Science*, *295*(5558), 1272–1275, doi:10.1126/science.1065080.

Shibata, T., H. Vömel, S. Hamdi, S. Kaloka, F. Hasebe, M. Fujiwara, and M. Shiotani (2007), Tropical cirrus clouds near cold point tropopause under ice supersaturated conditions observed by lidar and balloon-borne cryogenic frost point hygrometer, *J. Geophys. Res.*, *112*, D03210, doi:10.1029/2006JD007361.

Solomon, S., K. Rosenlof, R. Portmann, J. Daniel, S. Davis, T. Sanford, and G.-K. Plattner (2010), Contributions of stratospheric water vapor to decadal changes in the rate of global warming, *Science*, *327*, 1219–1223, doi:10.1126/science.1182488.

Uppala, S. M., et al. (2005), The ERA-40 re-analysis, *Q. J. R. Meteorol. Soc.*, *131*(612), 2961–3012.

Vömel, H., S. J. Oltmans, D. Kley, and P. J. Crutzen (1995a), New evidence for the stratospheric dehydration mechanism in the equatorial Pacific, *Geophys. Res. Lett.*, *22*(23), 3235–3238, doi:10.1029/95GL02940.

Vömel, H., S. Oltmans, D. Hofmann, T. Deshler, and J. Rosen (1995b), The evolution of the dehydration in the Antarctic stratospheric vortex, *J. Geophys. Res.*, *100*(D7), 13,919–13,926, doi:10.1029/95JD01000.

Vömel, H., et al. (2002), Balloon-borne observations of water vapor and ozone in the tropical upper troposphere and lower stratosphere, *J. Geophys. Res.*, *107*(D14), 4210, doi:10.1029/2001JD000707.

Vömel, H., M. Fujiwara, M. Shiotani, F. Hasebe, S. J. Oltmans, and J. E. Barnes (2003), The behavior of the Snow White chilled-mirror hygrometer in extremely dry conditions, *J. Atmos. Oceanic Technol.*, *20*(11), 1560–1567.

Vömel, H., et al. (2007a), Validation of Aura Microwave Limb Sounder water vapor by balloon-borne Cryogenic Frost point Hygrometer measurements, *J. Geophys. Res.*, *112*, D24S37, doi:10.1029/2007JD008698.

Vömel, H., H. Selkirk, L. Miloshevich, J. Valverde-Canossa, J. Valdés, E. Kyrö, R. Kivi, W. Stolz, G. Peng, and J.A. Diaz (2007b), Radiation dry bias of the Vaisala RS92 humidity sensor, *J. Atmos. Oceanic Technol.*, *24*(6), 953–963.

Vömel, H., V. Yushkov, S. Khaykin, L. Korshunov, E. Kyrö, and R. Kivi (2007c), Intercomparisons of stratospheric water vapor sensors: FLASH-B and NOAA/CMDL frost-point hygrometer, *J. Atmos. Oceanic Technol.*, *24*(6), 941–952.

Vömel, H., D. E. David, and K. Smith (2007d), Accuracy of tropospheric and stratospheric water vapor measurements by the cryogenic frost point hygrometer: Instrumental details and observations, *J. Geophys. Res.*, *112*, D08305, doi:10.1029/2006JD007224.

Waters, J. W., et al. (2006), The Earth Observing System Microwave Limb Sounder (EOS MLS) on the Aura satellite, *IEEE Trans. Geosci. Remote Sens.*, *44*(5), 1075–1092.

Wrotny, J. E., G. E. Nedoluha, C. Boone, G. P. Stiller, and J. P. McCormack (2010), Total hydrogen budget of the equatorial upper stratosphere, *J. Geophys. Res.*, *115*, D04302, doi:10.1029/2009JD012135.

Yamashita, Y., K. Sakamoto, H. Akiyoshi, M. Takahashi, T. Nagashima, and L. B. Zhou (2010), Ozone and temperature response of a chemistry climate model to the solar cycle and sea surface temperature, *J. Geophys. Res.*, doi:10.1029/2009JD013436, in press.

M. Fujiwara, F. Hasebe, and K. Shimizu, Graduate School of Environmental Science, Hokkaido University, N10 W5, Sapporo 060-0810, Japan. (fuji@ees.hokudai.ac.jp)

S. Iwasaki, National Defense Academy, Hashirimizu 1-10-20, Yokosuka 239-8686, Japan.

N. Nishi, Graduate School of Science, Kyoto University, Kyoto 606-8502, Japan.

S.-Y. Ogino, Japan Agency for Marine-Earth Science and Technology, Natsushima 2-15, Yokosuka 237-0061, Japan.

S. J. Oltmans, Global Monitoring Division, NOAA Earth System Research Laboratory, Boulder, CO 80305, USA.

H. B. Selkirk, Goddard Earth Sciences and Technology Center, University of Maryland Baltimore County, NASA Goddard Space Flight Center, Greenbelt, MD 20771, USA.

T. Shibata, Graduate School of Environmental Studies, Nagoya University, Nagoya 464-8601, Japan.

M. Shiotani and E. Nishimoto, Research Institute for Sustainable Humanosphere, Kyoto University, Gokasho, Uji 611-0011, Japan.

J. M. Valverde Canossa, Universidad Nacional, Heredia 86-3000, Costa Rica.

H. Vömel, Meteorologisches Observatorium Lindenberg, Deutscher Wetterdienst, D-15848 Tauche/Lindenberg, Germany.